

Effects of molecular noise on cell size control

Motasem ElGamel¹ and Andrew Mugler^{1,*}

¹*Department of Physics and Astronomy, University of Pittsburgh, Pittsburgh, Pennsylvania 15260, USA*

Cells employ control strategies to maintain a stable size. Dividing at a target size (the ‘sizer’ strategy) is thought to produce the tightest size distribution. However, this result follows from phenomenological models that ignore the molecular mechanisms required to implement the strategy. Here we investigate a simple mechanistic model for exponentially growing cells whose division is triggered at a molecular abundance threshold. We find that size noise inherits the molecular noise and is consequently minimized not by the sizer but by the ‘adder’ strategy, where a cell divides after adding a target amount to its birth size. We derive a lower bound on size noise that agrees with publicly available data from six microfluidic studies on *Escherichia coli* bacteria.

Maintaining a stable cell size is a central requirement of life. Fatal consequences to large cell size fluctuations include cytoplasm dilution [1] and impaired mitochondrial function [2]. Additionally, cell size is important for optimizing nutrient intake [3, 4], accommodating intracellular content [4, 5], maintaining uniformity in tissues [6], and more [7]. Size stability, in exponentially growing cells, does not emerge passively: because of unavoidable noise in growth and division, cells employ active size control strategies [3, 4, 6]. The strategy predicted to produce the tightest cell size distribution is known as the ‘sizer’ [8, 9]. In this strategy, a cell divides when a target size is reached, regardless of its birth size or the required growth time. Because the sizer attempts to reset the cell size every generation, it makes sense that this strategy would lead to minimal size noise. Yet, pure sizers are rarely observed in microbial growth control.

The prediction that a sizer has the lowest size noise is based on phenomenological models that ignore underlying molecular mechanisms [8, 10–12]. Dividing at a target size requires a molecular mechanism that tells the cell when the target is reached, and that mechanism may have its own noise that impacts size noise. Indeed, molecular noise has been shown to have important effects on cell size control, even in a high gene expression regime [13, 14]. Noise in the accumulation of a division-triggering molecule can explain the universality of size distributions in the ‘adder’ strategy [15], where a cell divides after adding a target amount to its birth size [8, 16–18]. Noise in the accumulation threshold itself contributes to size noise and can even alter the observed strategy among sizer, adder, and ‘timer’ (where a cell divides after a target time) [19]. Molecular noise in the DNA replication mechanism [20] or cell-to-cell variability [21] can make sizer control appear adder-like. Together, these works show that molecular noise has a driving impact on cell size control, but a simple and mechanistic understanding of its effects on cell size noise across the timer-adder-sizer spectrum remains elusive.

Here we introduce a mechanistic model of cell size control in which division occurs when a single molecular species (such as FtsZ [3, 22] or peptidoglycan [23]) accu-

mulates to an abundance threshold. The model admits the timer, adder, and sizer as limits, and we find that the variance in birth size is minimized by the adder, not the sizer. The reason is that the sizer mechanism requires active protein degradation in our model, resulting in high molecular noise for a fixed protein production cost, and this noise overpowers the sizer’s otherwise tight control. We predict a lower bound on size noise that is lowest for the adder and find agreement with publicly available data from six microfluidic studies on *Escherichia coli* bacteria.

We first summarize the prevailing phenomenological model of cell size control [8, 12]. The simplest form assumes that a cell grows exponentially at a constant rate and divides in half [Fig. 1(a)]. In the n th generation, a cell with birth size b_n and growth rate α has size

$$s_n(t) = b_n e^{\alpha t} \quad (1)$$

at time t . Denoting the division time as t_n , the new birth size is $b_{n+1} = b_n e^{\alpha t_n} / 2$. Defining $\epsilon_n = \ln(b_n / \bar{b})$ as the logarithmic deviation of the birth size from its long-time average, and $\delta_n = \alpha t_n - \ln 2$ as the deviation

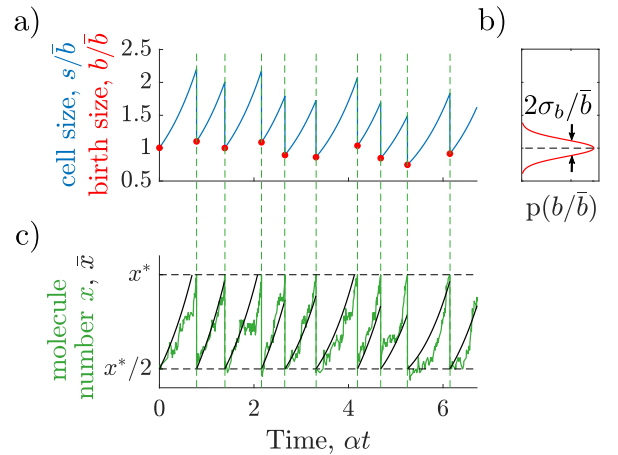


FIG. 1. (a) A cell grows exponentially and divides in half. (b) The birth size fluctuates. (c) Division occurs when a molecule reaches an abundance threshold. Noise in the molecule number contributes to noise in the birth size. Here $\gamma = 10^{-2}$, $\rho = 1$, and $k/\alpha = 50$.

of the exponential phase from its expected value for size doubling, this expression becomes

$$\epsilon_{n+1} = \epsilon_n + \delta_n. \quad (2)$$

If δ_n is independent of ϵ_n , then Eq. 2 describes a random walk, which is not stable. Therefore, most size control models assume that the phase corrects for deviations in the birth size [10, 12, 24],

$$\delta_n = -\beta\epsilon_n + \eta_n. \quad (3)$$

Here, the homeostasis parameter β sets the strength of the correction, and η_n is uncorrelated Gaussian noise. Eq. 3 ensures that cells born larger ($\epsilon_n > 0$) grow for less time ($\delta_n < 0$) on average.

The values $\beta = 0, 1/2$, and 1 correspond to the timer, adder, and sizer strategies, respectively [8, 12]. Correspondingly, β controls the noise in the birth size, σ_b^2/\bar{b}^2 [Fig. 1(b)]. Specifically, experiments in bacteria suggest $\sigma_b/\bar{b} \sim 20\%$ [22, 25–29], for which $\sigma_\epsilon^2 \approx \sigma_b^2/\bar{b}^2 \ll 1$. Inserting Eq. 2 into Eq. 3 and considering the variance obtains $\sigma_\epsilon^2 = (1 - \beta)^2\sigma_\epsilon^2 + \sigma_\eta^2$ in steady state. Solving for σ_ϵ^2 , we see that the size noise,

$$\frac{\sigma_b^2}{\bar{b}^2} \approx \sigma_\epsilon^2 = \frac{\sigma_\eta^2}{\beta(2 - \beta)}, \quad (4)$$

is minimized for the sizer at $\beta = 1$.

In Eq. 3, the homeostasis parameter β and the timing noise η_n are phenomenological, rather than arising from an underlying molecular mechanism. Our key advance will be to show that the mechanism that sets β also affects η_n , such that the two are not independent as commonly assumed. Instead, we will see that the coupling between β and η_n endows σ_ϵ^2 in Eq. 4 with an effective β dependence, opening the possibility that the sizer does not minimize size noise after all.

Consider a molecular species whose abundance x triggers cell division when it reaches a threshold x_* [Fig. 1(c)]. We intend this construction to be minimal and generic [15, 30], but we are also motivated by specific molecular species in bacteria such as FtsZ [3, 22] or peptidoglycan [23] that are thought to accumulate to a threshold amount to initiate division. We assume that the threshold is fixed and focus on the timing noise in reaching it, rather than preexisting noise in its value [19]. For simplicity we ignore the initiation of DNA replication, which is also thought to be an important trigger for cell division and can affect size control [20].

We prescribe the simplest possible reactions for x , namely linear production and degradation. We will see that allowing production to either scale with [22, 23] or be independent of cell size will allow the model to reduce to the timer, adder, and sizer strategies in particular limits. Thus, the dynamics of x within generation n are

$$\frac{d\bar{x}_n}{dt} = \nu + \mu s_n - \lambda \bar{x}_n, \quad (5)$$

where ν is the size-independent production rate, μs_n is the size-dependent production rate, λ is the degradation rate, and the bar denotes the fact that we will later be interested in the noise in x . Although Eq. 5 is not the only model that spans the timer-adder-sizer spectrum [31], we are motivated by experiments that specifically suggest that degradation [22] and size-proportional production [22, 23] are responsible for sizer and adder control, respectively, as we will see for our model below. For simplicity and consistency with the phenomenological model above, we neglect the effects of nonexponential growth [32, 33], heterogeneous growth rates [14, 34], and noisy [12] or asymmetric division [26, 35, 36] (although we relax the latter two assumptions later on). We further assume that x is initialized at $x_*/2$ each generation, corresponding to symmetric partitioning at division, although none of our conclusions change if instead x is initialized at zero, for example if the molecule is cleared or used in pole construction [23].

If $\mu = \lambda = 0$ in Eq. 5, then $\bar{x}_n(t) = x_*/2 + \nu t$, which reaches x_* in a constant time, corresponding to the timer strategy. If instead $\nu = \lambda = 0$, then $\bar{x}_n(t) = x_*/2 + \mu b_n(e^{\alpha t} - 1)/\alpha$ using Eq. 1. Solving the division condition $\bar{x}_n(t) = x_*$ for t and inserting it into Eq. 1 obtains $s_n = b_n + \alpha x_*/2\mu$, which shows that the cell adds a constant amount to its birth size—the adder strategy [22, 23]. Finally, if only $\nu = 0$, then Eq. 5 reads $d\bar{x}_n/dt = \mu s_n - \lambda \bar{x}_n$. If degradation is much faster than cell growth, $\lambda \gg \alpha$, then $s_n(t)$ is quasi-static on the response timescale of x , and $\bar{x}_n(t) \approx \mu s_n(t)/\lambda$. Thus, a molecule number threshold is equivalent to a size threshold, corresponding to the sizer strategy. These three limits suggest that we define two dimensionless parameters, $\gamma = \nu/\mu\bar{b}$ and $\rho = \lambda/\alpha$, for which the timer, adder, and sizer correspond to $\{\gamma \gg 1, \rho \ll 1\}$, $\{\gamma \ll 1, \rho \ll 1\}$, and $\{\gamma \ll 1, \rho \gg 1\}$, respectively, as illustrated by the icons in the corners of Fig. 2(a). For reference, a complete list of parameter definitions is given in [37].

In our model, the homeostasis parameter β defined by Eq. 3 is a function of the mechanistic parameters γ and ρ . To see this, we write the general solution to Eq. 5, $\bar{x}_n(t) = x_*e^{-\rho\alpha t}/2 + (k/\alpha)[(b_n/\bar{b})(e^{\alpha t} - e^{-\rho\alpha t})/(1 + \rho) + \gamma(1 - e^{-\rho\alpha t})/\rho]/(1 + \gamma)$. Here we have defined $k = \nu + \mu\bar{b}$ as the total molecule production rate. It represents the intrinsic biochemical rate at which a molecule is produced, and therefore we keep it fixed throughout. Fixing k is consistent with observed dependences of constitutive gene expression [38] (in the timer limit) and of balanced biosynthesis [22, 23] (in the adder limit) on the cell growth rate. Nevertheless, we find that our conclusions are unchanged if we instead fix the threshold x_* [37].

To find β from $\bar{x}_n(t)$, we again take $\epsilon_n = \ln(b_n/\bar{b})$ to be small, and we consider times t near division, where $\delta = \alpha t - \ln 2$ is expected to be small. We expand the

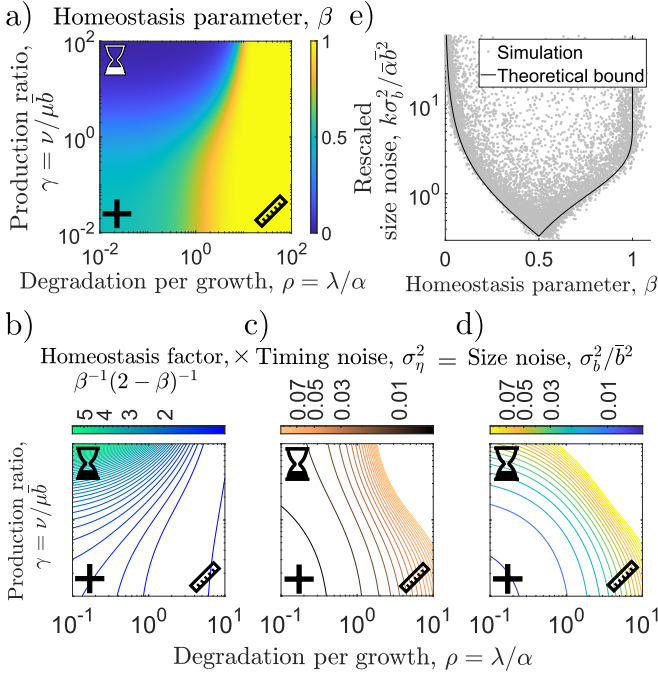


FIG. 2. (a) Homeostasis parameter β is a function of mechanistic parameters γ and ρ in our model. Symbols indicate limiting cases of timer (upper left), adder (lower left), and sizer (lower right). (b-d) Dependence of each component of the size noise on γ and ρ . (e) Rescaled size noise (CV^2) vs. homeostasis parameter β from simulations.

expression for $\bar{x}_n(t)$ to linear order in ϵ_n and δ as

$$\bar{x}_n(t) \approx c_0 + c_1\epsilon_n + c_2\delta, \quad (6)$$

where the expansion coefficients c_0 , c_1 , and c_2 are functions of x_* , γ , ρ , and k/α [37]. At division, we have $\bar{x}_n(t) = x_*$ and $\delta = \delta_n$. The constant terms in Eq. 6 then read $x_* = c_0$, which when solved for x_* obtains

$$x_* = 2 \left(\frac{k/\alpha}{1+\gamma} \right) \left[\frac{1}{1+\rho} + \frac{\gamma}{\rho} \left(\frac{r-1}{2r-1} \right) \right], \quad (7)$$

where $r \equiv 2^\rho$. Eq. 6 then reads $\delta_n = -(c_1/c_2)\epsilon_n$, which when compared with Eq. 3 implies

$$\beta = \frac{c_1}{c_2} = \frac{(2r-1)^2}{4r^2 + (g-2)r}, \quad (8)$$

where $g \equiv \gamma\rho + \gamma$, and the second step includes inserting Eq. 7 into the expression for c_2 . Eq. 8 is plotted in Fig. 2(a), and we see that, as expected, β approaches 0, 1/2, and 1 in the timer, adder, and sizer limits, respectively.

In principle, having calculated β for our model, Eq. 4 would then give the size noise. The factor $\beta^{-1}(2-\beta)^{-1}$ from Eq. 4, which we call the homeostasis factor, is plotted in Fig. 2(b), and we see that it is smallest for the sizer and largest for the timer, as commonly expected. However, thus far we have ignored noise in x . Noise in x

will propagate to noise in division timing and, in turn, to noise in cell size [15] [Fig. 1(c)]. To see this, we calculate in our model the statistics of the noise η_n defined by Eq. 3. Specifically, the timing noise is

$$\sigma_\eta^2 = \langle \sigma_{\delta_n|\epsilon_n}^2 \rangle \approx \left\langle \left(\frac{\partial \bar{x}_n}{\partial \delta} \Big|_{\delta=0} \right)^{-2} \sigma_{x_n|\epsilon_n}^2 \right\rangle = \frac{\langle \sigma_{x_n|\epsilon_n}^2 \rangle}{c_2^2}. \quad (9)$$

The first step follows from Eq. 3, conditioned on birth size, where the average is over birth size. The second step approximates the division noise (the noise in the first-passage time for x_n to reach x_*) by the molecule number noise, propagated via derivative. The third step takes this derivative from Eq. 6. We solve for the molecule number noise from the master equation [37] and find that it varies between the Poissonian limits of $\langle \sigma_{x_n|\epsilon_n}^2 \rangle = x_*/2$ for $\rho \ll 1$ and $\langle \sigma_{x_n|\epsilon_n}^2 \rangle = x_*$ for $\rho \gg 1$ [39]. Inserting it into Eq. 9 gives the timing noise, plotted in Fig. 2(c). We see that the timing noise is largest for the sizer. The reason is that the sizer requires strong degradation ($\rho \gg 1$), which, at a fixed production rate k , corresponds to fewer total molecules. Indeed, Eq. 7 shows that $x_* \rightarrow 0$ as $\rho \rightarrow \infty$. A lower threshold x_* is reached in fewer sequential steps, corresponding to larger timing noise.

The size noise is the product of the homeostasis factor and the timing noise (Eq. 4). Using Eqs. 8 and 9, $\sigma_b^2/\bar{b}^2 \approx \langle \sigma_{x_n|\epsilon_n}^2 \rangle / [c_1(2c_2 - c_1)]$. Inserting the molecule number noise and expansion coefficients and simplifying [37],

$$\frac{\sigma_b^2}{\bar{b}^2} = \frac{\alpha}{k} \left[\frac{(1+\gamma)(1+\rho)(2r^2-1)[(g+2\rho)r - (g+\rho)]}{\rho[8r^3 + 4(g-1)r^2 - 2(g+1)r + 1]} \right], \quad (10)$$

where again $r \equiv 2^\rho$ and $g \equiv \gamma\rho + \gamma$. Eq. 10 is plotted in Fig. 2(d), and we see that it is minimized for the adder. The reason is that the homeostasis factor is largest for the timer [Fig. 2(b)], whereas the timing noise is largest for the sizer [Fig. 2(c)], and this tradeoff makes their product smallest in between, for the adder. We have checked that Eqs. 8 and 10 agree with growth-and-division simulations, with division driven by stochastic reactions corresponding to the terms in Eq. 5 [40].

Because Eqs. 8 and 10 each depend on at least two parameters, there is no unique function relating the observables σ_b^2/\bar{b}^2 and β . However, there is a lower bound. The lower bound is obtained by solving Eq. 8 for γ , inserting the solution into Eq. 10, and minimizing with respect to ρ . We find numerically that the minimum corresponds to $\rho \rightarrow 0$ when $0 < \beta \leq 1/2$ and to $\gamma \rightarrow 0$ when $1/2 < \beta < 1$. In these limits, Eq. 10 becomes

$$\frac{\sigma_b^2}{\bar{b}^2} \geq \frac{\alpha/k}{\beta(2-\beta)} \begin{cases} (1-\beta)[\beta + (1-2\beta)\ln 2] & \beta \leq 1/2 \\ c(2\beta^2 - 4\beta + 1)\ln(1-\beta) & \beta > 1/2, \end{cases} \quad (11)$$

where $c \equiv (2\ln 2)^{-1}$. Eq. 11 is smallest for the adder ($\beta = 1/2$), giving $\sigma_b^2/\bar{b}^2 \geq \alpha/3k$. Eq. 11 also makes

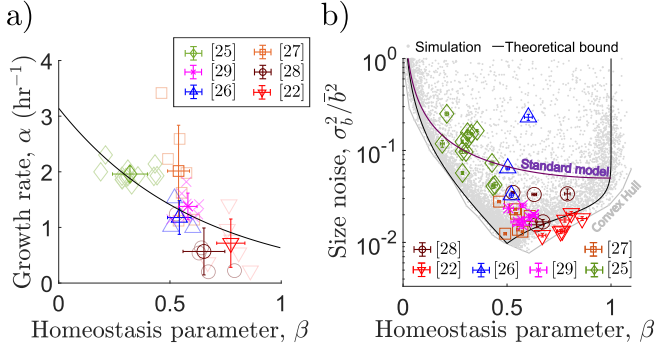


FIG. 3. (a) Growth rate α vs. homeostasis parameter β from publicly available data. Data fit to $\alpha(\beta) = 3.1 \exp(-1.6\beta)$ hr⁻¹ (black line). (b) Size noise (CV^2) vs. β from data in a, compared to theoretical lower bound (Eq. 11) and simulations, with $\alpha(\beta)$ inserted, and to the best-fit standard model (Eq. 4). In b, $k = 0.8/\text{min}$, set such that convex hull of simulation points first intersects the data.

clear that size noise decreases for smaller α or larger k , either of which allows more molecules to be produced in a generation. Finally, the denominator in Eq. 11 is the homeostasis factor $\beta^{-1}(2-\beta)^{-1}$. Comparing with Eq. 4, this fact makes clear that the molecular mechanism has endowed the timing noise σ_η^2 with a β dependence, i.e., the numerator in Eq. 11.

We test Eq. 11 against our simulations [37] in Fig. 2(e). Each point corresponds to a different value of γ , ρ and α/k , sampled uniformly in log space. We see that the simulated data points obey a lower bound on rescaled size noise $k\sigma_b^2/\alpha\bar{b}^2$ at each β value, in good agreement with Eq. 11, with minor discrepancy due to the approximations we made in Eqs. 6 and 9. We also test the robustness of our results to other typical noise sources, including growth rate variability, molecule partitioning noise, and noise in the molecular abundance threshold x^* [41] (Fig. S1 [37]). We find that adding noise sources generally increases size noise levels, as expected. Moreover, we find that noise in x^* , depending on the correlation time of fluctuations, can shift the data towards the timer (for large correlation time) or the sizer (for small correlation time), consistent with previous results [19]. In all cases, our predicted bound is obeyed, and a clear minimum in size noise exists away from the sizer.

Since Eq. 11 depends on α , to compare our theory with experiments, we must take the dependency of α on β into account. Because our theory does not probe α directly, but rather the ratio $\rho = \lambda/\alpha$, we rely on experimental data to determine the α - β relation empirically. Fig. 3(a) shows publicly available data from six microfluidic studies on *E. coli* [22, 25–29] (see [37] for data analysis). We see that β generally decreases with α across studies, a trend that is widely observed [10, 22, 28]. We fit the data in Fig. 3(a) to an exponentially decaying function, resulting in $\alpha = 3.1 \exp(-1.6\beta)$ hr⁻¹ (black line).

Inserting this dependence into Eq. 11 gives the lower bound shown in Fig. 3(b) (black line), along with the corresponding simulation data and their convex hull shown in gray. We compare this prediction to experimental size noise data from the same six studies. We see that the theory explains the data, specifically the strong fall-off of the size noise with β in the timer-adder region, the minimum near the adder, and the increase of noise with β in the adder-sizer region (in particular the data from [22], although more data would be needed at large β to verify this increase). In contrast, we see that the best fit of the standard model (Eq. 4, purple) fails to explain these features and is a poorer description of the data. Note that to set k in Eq. 11, we decrease it (thus increasing the predicted noise bound) until the simulation convex hull first intersects the data in Fig. 3(b). The resulting value of $k \approx 1/\text{min}$ is a plausible rate of protein production [42] and corresponds to a copy number of at least 50–500 molecules per cell [43]. Consistently, experimental estimates of the number of FtsZ proteins per cell are in the thousands [44].

We have demonstrated, using a minimal model of threshold-triggered division in bacteria, that cell size noise is minimized by the adder strategy, not the sizer strategy as conventionally expected. The reason is that molecular noise, missing in the conventional framework, amplifies size noise in the sizer limit, defined in our model by active protein degradation as suggested in experiments [22]. The amplification is due to high timing noise [Fig. 2(c, d)], consistent with recent related work [45]. Our predictions are supported by data from six studies in *E. coli* [22, 25–29] [Fig. 3(b)]. Specifically, we find that while the data span a range of β , for a given β most data lie close to the predicted noise bound, with exceptions that may be due to variations from other noise sources (Fig. S1 [37]). This suggests that size noise might not be minimized globally, but rather, for a given size control strategy, minimized for that strategy. Additionally, we predict that if cells are forced deeply into the sizer regime, either by slowing growth [22, 28] or perturbing degradation [22], size noise should increase, not decrease as predicted by the standard model [Fig. 3(b)].

Most bacteria exhibit adder control [11, 18, 26, 27], raising the question of whether the adder is optimal in some sense [45, 46]. Our model suggests that the adder, not the sizer, may provide the tightest attainable size control for bacteria. Other organisms show different size control mechanisms, with fission yeast, for example, exhibiting a strong sizer [47]. In fission yeast, division timing depends on a concentration threshold rather than a molecule number threshold as studied here [48]. We leave concentration-dependent size control for future work.

Our work emphasizes that the molecular mechanism underpins not only the size control strategy, but its statistics as well. Although we have focused on size noise in this work, we anticipate that this idea will have conse-

quences for other questions traditionally informed by a phenomenological understanding of size control, including multigenerational memory [49], cell geometry [21], population-level effects [50], and more.

We thank Hanna Salman and Fangwei Si for valuable discussions. This work was supported by National Science Foundation Grant Nos. PHY-2118561 and DMS-2245816.

* andrew.mugler@pitt.edu

- [1] Gabriel E Neurohr, Rachel L Terry, Jette Lengefeld, Megan Bonney, Gregory P Brittingham, Fabien Moretto, Teemu P Miettinen, Laura Pontano Vaites, Luis M Soares, Joao A Paulo, et al. Excessive cell growth causes cytoplasm dilution and contributes to senescence. *cell*, 176(5):1083–1097, 2019.
- [2] Teemu P Miettinen and Mikael Björklund. Cellular allometry of mitochondrial functionality establishes the optimal cell size. *Developmental cell*, 39(3):370–382, 2016.
- [3] An-Chun Chien, Norbert S Hill, and Petra Anne Levin. Cell size control in bacteria. *Current biology*, 22(9):R340–R349, 2012.
- [4] Jonathan J Turner, Jennifer C Ewald, and Jan M Skotheim. Cell size control in yeast. *Current biology*, 22(9):R350–R359, 2012.
- [5] Wallace F Marshall, Kevin D Young, Matthew Swaffer, Elizabeth Wood, Paul Nurse, Akatsuki Kimura, Joseph Frankel, John Wallingford, Virginia Walbot, Xian Qu, et al. What determines cell size? *BMC biology*, 10(1):1–22, 2012.
- [6] Miriam B Ginzberg, Ran Kafri, and Marc Kirschner. On being the right (cell) size. *Science*, 348(6236):1245075, 2015.
- [7] Kevin D Young. The selective value of bacterial shape. *Microbiology and molecular biology reviews*, 70(3):660–703, 2006.
- [8] Ariel Amir. Cell size regulation in bacteria. *Physical review letters*, 112(20):208102, 2014.
- [9] Giuseppe Facchetti, Fred Chang, and Martin Howard. Controlling cell size through sizer mechanisms. *Current Opinion in Systems Biology*, 5:86–92, 2017.
- [10] Yu Tanouchi, Anand Pai, Heungwon Park, Shuqiang Huang, Rumen Stamatov, Nicolas E Buchler, and Lingchong You. A noisy linear map underlies oscillations in cell size and gene expression in bacteria. *Nature*, 523(7560):357–360, 2015.
- [11] Lisa Willis and Kerwyn Casey Huang. Sizing up the bacterial cell cycle. *Nature Reviews Microbiology*, 15(10):606–620, 2017.
- [12] Lee Susman, Maryam Kohram, Harsh Vashistha, Jeffrey T Nechleba, Hanna Salman, and Naama Brenner. Individuality and slow dynamics in bacterial growth homeostasis. *Proceedings of the National Academy of Sciences*, 115(25):E5679–E5687, 2018.
- [13] Alberto Stefano Sassi, Mayra Garcia-Alcala, Maximino Aldana, and Yuhai Tu. Protein concentration fluctuations in the high expression regime: Taylor’s law and its mechanistic origin. *Physical review X*, 12(1):011051, 2022.
- [14] Kuheli Biswas and Naama Brenner. Cell-division time statistics from stochastic exponential threshold-crossing. *bioRxiv*, 2022.
- [15] Khem Raj Ghusinga, Cesar A Vargas-Garcia, and Abhyudai Singh. A mechanistic stochastic framework for regulating bacterial cell division. *Scientific reports*, 6(1):1–9, 2016.
- [16] L Sompayrac and O Maaløe. Autorepressor model for control of dna replication. *Nature New Biology*, 241(109):133–135, 1973.
- [17] WJ Voorn, LJH Koppes, and NB Grover. Mathematics of cell division in escherichia coli: comparison between sloppy-size and incremental-size kinetics. *Curr. Top. Mol. Gen.*, 1:187–194, 1993.
- [18] John T Sauls, Dongyang Li, and Suckjoon Jun. Adder and a coarse-grained approach to cell size homeostasis in bacteria. *Current opinion in cell biology*, 38:38–44, 2016.
- [19] Liang Luo, Yang Bai, and Xiongfei Fu. Stochastic threshold in cell size control. *Physical Review Research*, 5(1):013173, 2023.
- [20] Mareike Berger and Pieter Rein ten Wolde. Robust replication initiation from coupled homeostatic mechanisms. *Nature Communications*, 13(1):6556, 2022.
- [21] Giuseppe Facchetti, Benjamin Knapp, Fred Chang, and Martin Howard. Reassessment of the basis of cell size control based on analysis of cell-to-cell variability. *Biophysical journal*, 117(9):1728–1738, 2019.
- [22] Fangwei Si, Guillaume Le Treut, John T Sauls, Stephen Vadia, Petra Anne Levin, and Suckjoon Jun. Mechanistic origin of cell-size control and homeostasis in bacteria. *Current Biology*, 29(11):1760–1770, 2019.
- [23] Leigh K Harris and Julie A Theriot. Relative rates of surface and volume synthesis set bacterial cell size. *Cell*, 165(6):1479–1492, 2016.
- [24] Matteo Osella, Eileen Nugent, and Marco Cosentino Lagomarsino. Concerted control of escherichia coli cell division. *Proceedings of the National Academy of Sciences*, 111(9):3431–3435, 2014.
- [25] Ping Wang, Lydia Robert, James Pelletier, Wei Lien Dang, Francois Taddei, Andrew Wright, and Suckjoon Jun. Robust growth of escherichia coli. *Current biology*, 20(12):1099–1103, 2010.
- [26] Manuel Campos, Ivan V Surovtsev, Setsu Kato, Ahmad Paintdakhi, Bruno Beltran, Sarah E Ebmeier, and Christine Jacobs-Wagner. A constant size extension drives bacterial cell size homeostasis. *Cell*, 159(6):1433–1446, 2014.
- [27] Sattar Taheri-Araghi, Serena Bradde, John T Sauls, Norbert S Hill, Petra Anne Levin, Johan Paulsson, Massimo Vergassola, and Suckjoon Jun. Cell-size control and homeostasis in bacteria. *Current biology*, 25(3):385–391, 2015.
- [28] Mats Wallden, David Fange, Ebba Gregorsson Lundius, Özden Baltekin, and Johan Elf. The synchronization of replication and division cycles in individual e. coli cells. *Cell*, 166(3):729–739, 2016.
- [29] Harsh Vashistha, Maryam Kohram, and Hanna Salman. Non-genetic inheritance restraint of cell-to-cell variation. *Elife*, 10:e64779, 2021.
- [30] RM Teather, JF Collins, and WD Donachie. Quantal behavior of a diffusible factor which initiates septum formation at potential division sites in escherichia coli. *Journal of bacteriology*, 118(2):407–413, 1974.

- [31] César Nieto, Juan Arias-Castro, Carlos Sánchez, César Vargas-García, and Juan Manuel Pedraza. Unification of cell division control strategies through continuous rate models. *Physical Review E*, 101(2):022401, 2020.
- [32] Prathitha Kar, Sriram Tiruvadi-Krishnan, Jaana Männik, Jaan Männik, and Ariel Amir. Distinguishing different modes of growth using single-cell data. *Elife*, 10, 2021.
- [33] Arianna Cylke and Shiladitya Banerjee. Super-exponential growth and stochastic size dynamics in rod-like bacteria. *Biophysical Journal*, 122(7):1254–1267, 2023.
- [34] Maryam Kohram, Harsh Vashistha, Stanislas Leibler, BingKan Xue, and Hanna Salman. Bacterial growth control mechanisms inferred from multivariate statistical analysis of single-cell measurements. *Current Biology*, 31(5):955–964, 2021.
- [35] Srividya Iyer-Biswas, Charles S Wright, Jonathan T Henry, Klevin Lo, Stanislav Burov, Yihan Lin, Gavin E Crooks, Sean Crosson, Aaron R Dinner, and Norbert F Scherer. Scaling laws governing stochastic growth and division of single bacterial cells. *Proceedings of the National Academy of Sciences*, 111(45):15912–15917, 2014.
- [36] Felix Barber, Jiseon Min, Andrew W Murray, and Ariel Amir. Modeling the impact of single-cell stochasticity and size control on the population growth rate in asymmetrically dividing cells. *PLoS Computational Biology*, 17(6):e1009080, 2021.
- [37] See Supplemental Material for additional derivations, stochastic simulations, and analysis of published experimental data.
- [38] Stefan Klumpp and Terence Hwa. Bacterial growth: global effects on gene expression, growth feedback and proteome partition. *Current opinion in biotechnology*, 28:96–102, 2014.
- [39] For $\rho \ll 1$, degradation is negligible, meaning that $x_*/2$ production events are required to take the molecule number from the initial condition of $x_*/2$ to the threshold of x_* . This is a Poisson birth process with variance $\sigma_x^2 = x_*/2$. For $\rho \gg 1$, strong degradation quickly erases memory of the initial condition, and production and degradation proceed until the threshold x_* is reached. This is a Poisson birth-death process with variance $\sigma_x^2 = x_*$.
- [40] Daniel T Gillespie. Exact stochastic simulation of coupled chemical reactions. *The journal of physical chemistry*, 81(25):2340–2361, 1977.
- [41] Saurabh Modi, Cesar Augusto Vargas-Garcia, Khem Raj Ghusinga, and Abhyudai Singh. Analysis of noise mechanisms in cell-size control. *Biophysical journal*, 112(11):2408–2418, 2017.
- [42] David Kennell and Howard Riezman. Transcription and translation initiation frequencies of the escherichia coli lac operon. *Journal of molecular biology*, 114(1):1–21, 1977.
- [43] In the adder limit, Eq. 7 reads $x_* = 2k/\alpha$. For growth rates in the range 0.25–2.5/hr [Fig. 3(a)], the value of $k \approx 1/\text{min}$ in Fig. 3(b) corresponds to $x_* \approx 50$ –500. Given that our model neglects details of the bacterial division process that likely add noise, this range is expected to be an underestimate.
- [44] Andrea Feucht, Isabelle Lucet, Michael D Yudkin, and Jeffery Errington. Cytological and biochemical characterization of the ftsa cell division protein of bacillus subtilis. *Molecular microbiology*, 40(1):115–125, 2001.
- [45] Felix Proulx-Giraldeau, Jan M Skotheim, and Paul François. Evolution of cell size control is canalized towards adders or sizers by cell cycle structure and selective pressures. *Elife*, 11:e79919, 2022.
- [46] Jie Lin and Ariel Amir. The effects of stochasticity at the single-cell level and cell size control on the population growth. *Cell systems*, 5(4):358–367, 2017.
- [47] A Sveczer, B Novak, and JM Mitchison. The size control of fission yeast revisited. *Journal of cell science*, 109(12):2947–2957, 1996.
- [48] Elizabeth Wood and Paul Nurse. Sizing up to divide: mitotic cell-size control in fission yeast. *Annual review of cell and developmental biology*, 31:11–29, 2015.
- [49] Motasem ElGamel, Harsh Vashistha, Hanna Salman, and Andrew Mugler. Multigenerational memory in bacterial size control. *Phys. Rev. E*, 108:L032401, 2023.
- [50] Ethan Levien, Jiseon Min, Jane Kondev, and Ariel Amir. Non-genetic variability in microbial populations: survival strategy or nuisance? *Reports on Progress in Physics*, 84(11):116601, 2021.

SUPPLEMENTAL MATERIAL

Variables		Parameters		Defined quantities	
t	Time	α	Cell growth rate	$\epsilon_n \equiv \ln(b_n/\bar{b})$	Scaled, zero-mean birth size
n	Generation	β	Homeostasis parameter	$\delta_n \equiv \alpha t_n - \ln 2$	Scaled, zero-mean division time
b_n	Cell birth size	ν	Size-independent production rate	$\gamma \equiv \nu/\mu\bar{b}$	Production rate ratio
t_n	Cell division time	μ	Size-dependent production rate	$\rho \equiv \lambda/\alpha$	Degradation per growth
$s_n(t)$	Cell size	λ	Degradation rate	$k \equiv \nu + \mu\bar{b}$	Total production rate
$x_n(t)$	Molecule number	x_*	Molecule number threshold	$r \equiv 2^\rho, g \equiv \gamma\rho + \gamma$	For notational convenience

TABLE S1. Symbols used in this study.

MASTER EQUATION AND GENERATING FUNCTION

Eqs. 1 and 5 define the average dynamics of our model. With size growing exponentially with rate α and protein number x growing scholastically with birth and death rates, $\nu + \mu s$ and λx respectively. Our goal is to find the effect of intrinsic molecular noise on size statistics. We start by writing the birth-death master equation for x

$$\partial_t p(x, t) = t^+(x-1)p(x-1, t) + t^-(x+1)p(x+1, t) - (t^+(x) + t^-(x))p(x, t), \quad (\text{S1})$$

where $t^+(x)$ and $t^-(x)$ are the transition rates for the processes $x \rightarrow x+1$ and $x \rightarrow x-1$ respectively. The transition rates can be read off from Eq. 5 to be

$$\begin{aligned} t^+(x) &= \nu + \mu s, \\ t^-(x) &= \lambda x, \end{aligned} \quad (\text{S2})$$

and Eq. S1 becomes

$$\partial_t p(x, t) = (\nu + \mu s)p(x-1, t) + \lambda(x+1)p(x+1, t) - (\nu + \mu s + \lambda x)p(x, t). \quad (\text{S3})$$

After inserting the solution for Eq. 1, we get

$$\partial_t p(x, t) = (\nu + \mu b_n e^{\alpha t})p(x-1, t) + \lambda(x+1)p(x+1, t) - (\nu + \mu b_n e^{\alpha t} + \lambda x)p(x, t). \quad (\text{S4})$$

We define a generating function $G(s, t)$ as

$$G(s, t) = \sum_{x=0} s^x p(x, t), \quad (\text{S5})$$

then, differentiate w.r.t time

$$\partial_t G(s, t) = \sum_{x=0} s^x \partial_t p(x, t). \quad (\text{S6})$$

Substituting Eq. S1 in S6, we get

$$\partial_t G(s, t) = \sum_{x=0} s^x [(\nu + \mu b_n e^{\alpha t})p(x-1, t) + \lambda(x+1)p(x+1, t) - (\nu + \mu b_n e^{\alpha t} + \lambda x)p(x, t)]. \quad (\text{S7})$$

Each term in the RHS of Eq. S7 can be rewritten as

$$\sum_{x=0} s^x p(x-1, t) = \sum_{x=1} s^x p(x-1, t) = \sum_{x=0} s^{x+1} p(x, t) = sG(s, t), \quad (\text{S8})$$

$$\sum_{x=0} s^x (x+1)p(x+1, t) = \sum_{x=1} s^{x-1} x p(x, t) = \partial_s \sum_{x=1} s^x p(x, t) = \partial_s \left[\sum_{x=0} s^x p(x, t) - p(0, t) \right] = \partial_s G(s, t), \quad (\text{S9})$$

$$\sum_{x=0} s^x x p(x, t) = s \partial_s \sum_{x=0} s^x p(x, t) = s \partial_s G(s, t), \quad (\text{S10})$$

where the boundary condition $p(x < 0, t) = 0$ is assumed. Therefore, Eq. S7 becomes

$$\begin{aligned}\partial_t G(s, t) &= (\nu + \mu b_n e^{\alpha t}) s G(s, t) + \lambda \partial_s G(s, t) - (\nu + \mu b_n e^{\alpha t}) G(s, t) - \lambda s \partial_s G(s, t) \\ &= (\nu + \mu b_n e^{\alpha t})(s - 1) G(s, t) - \lambda(s - 1) \partial_s G(s, t).\end{aligned}\quad (\text{S11})$$

The solution to this PDE is

$$G(s, t) = \exp\left(\frac{s\nu}{\lambda} + \frac{e^{\alpha t} b_n \mu (s - 1)}{\lambda + \alpha}\right) F\left(t + \frac{1}{\lambda} \ln \frac{1}{s - 1}\right), \quad (\text{S12})$$

where F is an unknown function. Since at $t = 0$, molecules number $x(0) = x_0$, the distribution of x at $t = 0$ is $p(x, 0) = \delta_{xx_0}$. Thus, the condition

$$G(s, 0) = \sum_{x=0} s^x \delta_{xx_0} = s^{x_0}, \quad (\text{S13})$$

which enables us to find F ,

$$F\left(\frac{1}{\lambda} \ln \frac{1}{s - 1}\right) = s^{x_0} \exp\left(\frac{-s\nu}{\lambda} + \frac{b_n \mu (1 - s)}{\lambda + \alpha}\right). \quad (\text{S14})$$

we define the parameter $s' = \frac{1}{\lambda} \ln \frac{1}{s - 1}$ and solve for s in terms of s' to find $F(s')$, resulting in

$$F(s') = (1 + e^{-s'\lambda})^{x_0} \exp\left(\frac{-\nu}{\lambda} (1 + e^{-s'\lambda}) - \frac{b_n \mu e^{-s'\lambda}}{\lambda + \alpha}\right). \quad (\text{S15})$$

Hence,

$$F\left(t + \frac{1}{\lambda} \ln \frac{1}{s - 1}\right) = (1 + e^{-\lambda t} (s - 1))^{x_0} \exp\left(\frac{-\nu}{\lambda} (1 + e^{-\lambda t} (s - 1)) - \frac{b_n \mu e^{-\lambda t} (s - 1)}{\lambda + \alpha}\right), \quad (\text{S16})$$

which when plugged in S12 gives us the full solution for the generating function

$$G(s, t) = \exp\left(\frac{b_n \mu (s - 1)}{\lambda + \alpha} (e^{\alpha t} - e^{-\lambda t}) + \frac{\nu}{\lambda} (s - 1 - e^{-\lambda t} (s - 1))\right) (1 + e^{-\lambda t} (s - 1))^{x_0}. \quad (\text{S17})$$

MOLECULAR NOISE

Now that we derived the generating function, we can use it to derive the moments for x . The first and second moments can be derived using the generating function as follows

$$\partial_s G(s, t) = \sum_{x=0} x s^{x-1} p(x, t), \quad (\text{S18})$$

$$\partial_s^2 G(s, t) = \sum_{x=0} x(x - 1) s^{x-2} p(x, t), \quad (\text{S19})$$

for $s = 1$ this becomes

$$\partial_s G(s, t)|_{s=1} = \sum_{x=0} x p(x, t) = \langle x \rangle, \quad (\text{S20})$$

$$\partial_s^2 G(s, t)|_{s=1} = \sum_{x=0} x(x - 1) p(x, t) = \sum_{x=0} x^2 p(x, t) - \sum_{x=0} x p(x, t) = \langle x^2 \rangle - \langle x \rangle. \quad (\text{S21})$$

Thus, the variance given by

$$\sigma_x^2 = \langle x^2 \rangle - \langle x \rangle^2 = \partial_s^2 G(s, t)|_{s=1} + \partial_s G(s, t)|_{s=1} - (\partial_s G(s, t)|_{s=1})^2, \quad (\text{S22})$$

which results in

$$\sigma_{x|b_n}^2 = \frac{e^{-2\lambda t}}{\lambda(\lambda + \alpha)} \left[x_0(\lambda^2 + \alpha\lambda)(e^{\lambda t} - 1) + (\alpha\nu + \lambda\nu)e^{\lambda t}(e^{\lambda t} - 1) + \lambda b_n \mu e^{\lambda t}(e^{(\lambda + \alpha)t} - 1) \right]. \quad (\text{S23})$$

We use rescaled parameters defined in table S1, Eq. S23 becomes

$$\sigma_{x|b_n}^2 = \frac{e^{-2\rho\alpha t}}{\rho(\rho + 1)} \left[x_0(\rho + \rho^2)(e^{\rho\alpha t} - 1) + \frac{k}{\alpha} \frac{\gamma}{1 + \gamma} (1 + \rho)e^{\rho\alpha t}(e^{\rho\alpha t} - 1) + \rho b_n \frac{k}{\alpha} \frac{1}{(1 + \gamma)} e^{\rho\alpha t}(e^{(\rho + 1)\alpha t} - 1) \right]. \quad (\text{S24})$$

HOMEOSTASIS PARAMETER β

Next, we consider times t near division and write the expression for $\bar{x}_n(t)$ in the main text in terms of, $\delta = \alpha t - \ln 2$ and $\epsilon_n = \ln(b_n/\bar{b})$, the deviations from the average division phase αt and the average birth size respectively, and expand to first order in ϵ_n and δ . We find

$$\begin{aligned}\bar{x}_n(\delta) &= x_0 2^{-\rho}(1 - \rho\delta) + \frac{k\gamma}{\alpha\rho(1+\gamma)}[1 - 2^{-\rho}(1 - \rho\delta)] + \frac{k(1+\epsilon_n)}{\alpha(1+\gamma)(1+\rho)}[2(1+\delta) - 2^{-\rho}(1 - \rho\delta)] \\ &\approx c_0 + c_1\epsilon_n + c_2\delta,\end{aligned}\tag{S25}$$

where $x_0 = x_*/2$, x_* is the abundance threshold, $c_0 = x_0 2^{-\rho} + k\gamma[\alpha\rho(1+\gamma)]^{-1}[1 - 2^{-\rho}] + k[\alpha(1+\gamma)(1+\rho)]^{-1}[2 - 2^{-\rho}]$, $c_1 = k[\alpha(1+\gamma)(1+\rho)]^{-1}[2 - 2^{-\rho}]$ and $c_2 = k\gamma 2^{-\rho}[\alpha(1+\gamma)]^{-1} + k[\alpha(1+\gamma)(1+\rho)]^{-1}[2 + \rho 2^{-\rho}] - x_0 \rho 2^{-\rho}$. At division, we define $\delta = \delta_n$ and take the average of Eq. S25, we find $c_0 = x_*$, and Eq. S25 becomes,

$$\bar{x}_n(\delta) \approx x_* + c_1\epsilon_n + c_2\delta_n.\tag{S26}$$

Consequently, Eq. S26 at division reads

$$0 \approx c_1\epsilon_n + c_2\delta_n,\tag{S27}$$

which, when compared to Eq. 3 without the noise, reads

$$\beta = \frac{c_1}{c_2} = \frac{(2r-1)^2}{4r^2 + (g-2)r},\tag{S28}$$

where $g = \gamma\rho + \gamma$ and $r = 2^\rho$. Now we have a definition of β in terms of our model parameters which allows us to understand the mapping of our model dynamics to different homeostasis regimes.

SIZE NOISE

Noise in the growth factor at division, δ_n , “timing noise” is directly contributing to size noise from Eq. 4. The effect of molecule number noise on size noise can be seen directly from its relation to timing noise given by Eq. 9. To derive Eq. 9, we invoke the approximation $\sigma_{\delta_n|\epsilon_n}^2 \approx \left(\left.\frac{\partial \bar{x}_n}{\partial \delta_n}\right|_{\delta_n=0}\right)^{-2} \sigma_{x_n|\epsilon_n}^2$, which assumes that higher order terms of δ_n are negligible, or equivalently growth factors at division are tightly distributed around the average. We should also indicate that the timing noise for the population is the average of the noise in the growth factor over size. This results in

$$\sigma_\eta^2 = \langle \sigma_{\delta_n|\epsilon_n}^2 \rangle \approx \left\langle \left(\left. \frac{\partial \bar{x}_n}{\partial \delta} \right|_{\delta=0} \right)^{-2} \sigma_{x_n|\epsilon_n}^2 \right\rangle.\tag{S29}$$

From Eq. S26 we find $\left(\left.\frac{\partial \bar{x}_n}{\partial \delta}\right|_{\delta=0}\right)^{-2} = 1/c_2^2$, and Eq. S29 becomes

$$\sigma_\eta^2 \approx \frac{\langle \sigma_{x_n|\epsilon_n}^2 \rangle}{c_2^2}.\tag{S30}$$

The noise $\sigma_{x_n|\epsilon_n}^2$ can be found by writing down Eq. S24 in terms of ϵ_n and δ_n , which we find to be

$$\sigma_{x|\epsilon_n}^2 = c_1\epsilon_n + (c_2 + 2\rho x_0 2^{-2\rho})\delta_n + x_* - x_0 2^{-2\rho},\tag{S31}$$

given that $\langle \epsilon_n \rangle = 0$ and $\langle \delta_n \rangle = 0$, Eq. S30 becomes

$$\sigma_\eta^2 \approx \frac{x_* - x_0 2^{-2\rho}}{c_2^2}.\tag{S32}$$

Substituting Eqs. S32 and 8 in Eq. 4, size noise becomes

$$\frac{\sigma_b^2}{\bar{b}^2} \approx \sigma_\epsilon^2 = \frac{x_* - x_0 2^{-2\rho}}{c_1(2c_2 - c_1)}.\tag{S33}$$

We found numerically that the curve of minimum size noise is parametrized by $\rho \rightarrow 0$ when $0 < \beta \leq 1/2$ and $\gamma \rightarrow 0$ when $1/2 < \beta < 1$. To find the theoretical bound on size noise, we solve Eq. S28 in each branch for the other non-zero parameter in terms of β . This gives us

$$\rho \rightarrow 0, \gamma \rightarrow \frac{1}{\beta} - 2, \beta \leq 1/2 \quad (\text{S34})$$

$$\rho \rightarrow \frac{\ln(1/(1-\beta))}{\ln 2} - 1, \gamma \rightarrow 0, \beta > 1/2 \quad (\text{S35})$$

which when combined with Eq. S33 results in the final equation for the theoretical noise bound,

$$\frac{\sigma_b^2}{\bar{b}^2} \geq \frac{\alpha/k}{\beta(2-\beta)} \begin{cases} (1-\beta)[\beta + (1-2\beta)\ln 2] & \beta \leq 1/2 \\ c(2\beta^2 - 4\beta + 1)\ln(1-\beta) & \beta > 1/2. \end{cases} \quad (\text{S36})$$

SIMULATION AND DATA ANALYSIS

We simulated the stochastic dynamics of x using the stochastic simulation algorithm, then calculated the size noise and homeostasis parameter β . Each point in the simulation shown in Fig. 2(e) corresponds to a different value of γ , ρ , and α/k , sampled uniformly in log space. We expect our simulation to obey the theoretical bound with some deviation instances due to the approximations we made in Eqs. 6 and 9.

We performed analysis on publicly available from six microfluidic studies on *E. coli* referenced in the main text. All data sets typically contained size, time and growth rate measurements. In references [25, 29], where the available data did not contain rate measurements, we calculated α for each generation by assuming exponential growth of cells [Eq. 1]. Solving for α , we find the relation

$$\alpha = \frac{1}{T} \ln \frac{s_n(T)}{b_n}, \quad (\text{S37})$$

where T is generational time, $s_n(T)$ is division size, and b_n is birth size. To obtain the value of β from experiments we performed linear regression analysis using ϵ_n and δ_n calculated from data. According to Eq. 3, β is the negative value of the resulting slope.

Error bars in all figures represent standard error (SE) in the data. For α , SE was obtained directly from the data by calculating σ_α/\sqrt{n} . In the case of β , SE was calculated for the fit using MATLAB. In order to calculate SE for the CV^2 (σ_b^2/\bar{b}^2) in Fig. 3(b), we performed bootstrapping on the data. For each data set, we randomly sampled N data points that we used to calculate σ_b^2/\bar{b}^2 starting from $N = 5$. We then repeated the random sampling 50 times for the same N and calculated SE for the obtained 50 values of σ_b^2/\bar{b}^2 . After that, we increased the value of N gradually and repeated the procedure, eventually we could interpolate the SE value for the total number of available data points.

EXTRINSIC NOISE SOURCES

Other sources of noise are expected to affect the distribution and contribute to noise. We tested the robustness of our results to three noise sources: (1) growth rate noise, (2) partitioning noise of the size control molecules upon division, and (3) noise in the copy-number threshold that initiates division. We again used the stochastic simulation algorithm to simulate the stochastic dynamics of accumulation of the size control molecule. Results are shown in Fig. S1.

Noise in the growth rate was sampled each generation and simulated as a gaussian white noise with noise strength of 20% of the average, with noise strength chosen consistently with the experimental data (see Fig. 3 a). The partitioning noise was simulated by distributing molecules upon division according to a binomial distribution between the two daughter cells. Copy number threshold noise was accounted for as intrinsic fluctuations with a given correlation time, which we varied, and simulated using the stochastic simulation algorithm.

We find that including all noise sources does not change the main results of our model, namely, the existence of a minimum size noise boundary, and a globally minimum size noise that is away from the sizer in contrast to the standard model (see Fig. S1). We found that, depending on the correlation time of the fluctuations in the division threshold, data will shift more towards the timer (high correlation time) or the sizer (small correlation time). This

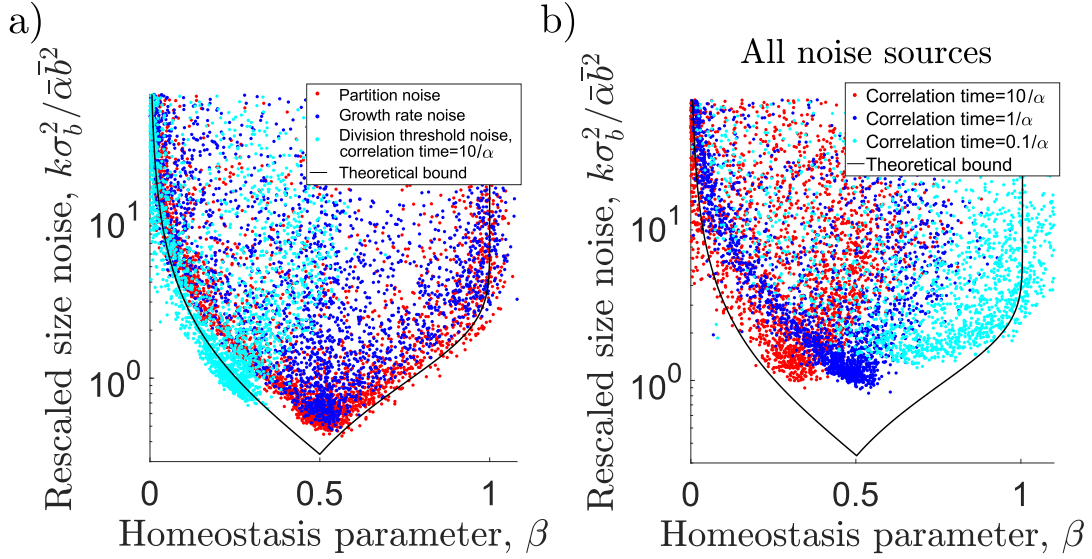


FIG. S1. (a) Rescaled size noise (CV^2) vs. homeostasis parameter β from simulations showing the effect of individual extrinsic source of noise. (b) The effect of all sources of noise combined on size noise.

observation is consistent with the results reported before in [19]. In all cases, our predicted bound was obeyed, with the simulation data tending to increase upon adding more noise sources. In all cases, a clear minimum robustly existed for the size noise, away from the sizer.

FIXING x_* INSTEAD OF k

For quantity-based mechanisms, where a component must reach a threshold, the sizer limit is achieved by making the degradation of that component much faster than the growth of the cell, so that the component tracks the cell volume at all times. To compensate for the fast degradation, either the production of the component must be high, or the threshold must be low. In our model, we assume a fixed cost (constant k), therefore, $x^* \rightarrow 0$ as $\beta \rightarrow 1$. If we relax this assumption and instead require that x^* is the fixed quantity, production k will change with β to meet the threshold, signifying different resource allocation. Using Eqs. 7, S34, and S35, we find k , for a fixed x^* , to be

$$k = \frac{x^* \alpha}{2} \begin{cases} (1 - \beta)/(\beta + \ln 2 - 2\beta \ln 2) & \beta \leq 1/2 \\ \ln[(1 - \beta)^{-1}]/\ln 2 & \beta > 1/2. \end{cases} \quad (\text{S38})$$

We can derive the size noise under the fixed x^* assumption by substituting Eq. S38 in Eq. 11, we find

$$\frac{\sigma_b^2}{\bar{b}^2} \geq \frac{1}{x^* \beta (2 - \beta)} \begin{cases} 2(\beta + \ln 2(1 - 2\beta))^2 & \beta \leq 1/2 \\ (4\beta - 2\beta^2 - 1) & \beta > 1/2. \end{cases} \quad (\text{S39})$$

Eq. S39 is plotted in Fig. S2, and it shows that while the size noise no longer diverges at the sizer limit ($\beta = 1$), it still increases monotonically in going from the adder ($\beta = 1/2$) to the sizer. The reason is that, while the standard model would predict a decrease in the size noise according to the homeostasis factor $H(\beta) = \beta^{-1}(2 - \beta)^{-1}$ (Fig. 2b), this decrease is outweighed by an increase in the molecule number noise from $x^*/2$ to x^* (described after Eq. 9). Specifically, from adder to sizer, the former effect decreases size noise by $H(1)/H(1/2) = 3/4$, while the latter effect increases size noise by $x^*/(x^*/2) = 2$.

Eq. S38 also shows that a fixed threshold implies a large production rate in the sizer limit. We see that for a pure sizer ($\beta = 1$) k is infinite, but even near the sizer it can be large. For example, taking a conservative value of the growth rate from Fig 3a, $\alpha \approx 0.5/hr$, and taking the estimate $x^* \approx 5000$ for the candidate accumulator protein FtsZ ([44], Table 1), we obtain $k \approx 20/min$ for the adder ($\beta = 1/2$). This value already matches the typical rates of transcription initiation and translation initiation in E. coli, both around 20/min ([42], Table 2). As we approach the sizer, the production rate increases: for $\beta = 0.9$ we have $k \approx 70/min$, and for $\beta = 0.99$ we have $k \approx 140/min$. Thus,

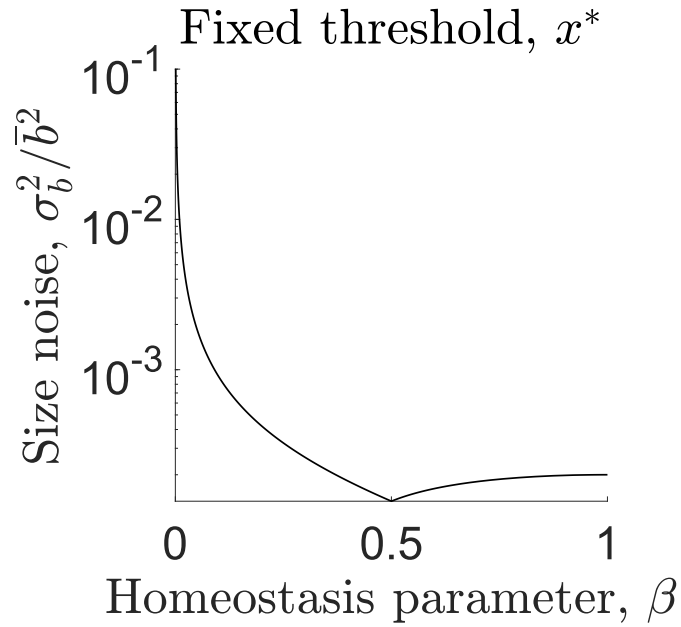


FIG. S2. Minimum size noise vs β for a fixed threshold $x^* = 5000$. The global minimum is still at the adder ($\beta = 1/2$).

we can see that under the fixed-threshold hypothesis, a sizer strategy could easily require a protein production rate that exceeds the limits set by the basic constraints of transcription and translation.

In summary, by fixing the protein abundance threshold rather than the protein production rate, we find that: 1) a qualitative minimum at $\beta = 1/2$ still holds, and 2) the protein production rate required to achieve sizer control ($\beta \rightarrow 1$) can readily exceed the fundamental speed limit of transcription and translation. Quantitatively, Fig. S2 shows that the minimum at $\beta = 1/2$ is shallow at larger β . Thus, on the basis of (1) alone, it could be concluded that $0.5 < \beta < 1$ is largely equivalent from a noise perspective, and that requirements other than noise minimization may set the value of β within this range. Nonetheless, it remains true that (2) is a fundamental observation about protein production limits and is sufficient to suggest that a pure sizer is unlikely to be achieved under a constant threshold protocol. In general, we conclude that our main finding, that size noise is not minimized by the sizer strategy, is robust to the precise optimization protocol.